Colloid and Polymer Science (2022) 300:1257–1267
https://doi.org/10.1007/s00396-022-05000-1

ORIGINAL CONTRIBUTION

Cryogenic transmission electron microscopy for observation of monomer protrusions that emerge during formation of dumbbell-shaped polymer colloids

Rouven Stuckert[1] · Marina Krumova[2] · Alexander Wittemann[1]

Received: 9 March 2022 / Revised: 1 June 2022 / Accepted: 16 June 2022 / Published online: 30 June 2022

Abstract
Anisotropic particles exhibit directional interactions resulting in a rich phase behavior. Considerable efforts have thus been invested in guiding particle synthesis into an anisotropic direction. Dumbbell-shaped polymer particles are one of the most remarkable examples. They result from phase separation during seeded polymerization. The underlying mechanism and thermodynamic principles are understood from its proximal end. Segregation of monomer and seed particle results in a monomer protrusion attached to the seed. Polymerization of the protrusion finally yields particles with two bulb-shaped halves. Little attention has been paid to an investigation of transient states, namely the formation of liquid protrusions grown from monomer-swollen seeds. This study demonstrates that cryogenic transmission electron microscopy is an excellent tool for mapping transient states within colloidal objects. Swelling of polymer particles and formation of liquid protrusions mediated by a surface coating on the seeds is explored for styrene and methyl-methacrylate at different temperatures and monomer-to-seed volume ratios.

Keywords Seeded polymerization · Dumbbell particles · Electron microscopy · Swelling · Monomer droplets · Phase separation

Introduction

If one aims to understand the synthesis of nanoparticles, it is often necessary to capture transient states of growth during their formation. This is particularly true in the case of anisotropic particles with shapes that are clearly distinctive from a spherical geometry, which is normally assumed due to minimization of surface tension. In the case of polymer particles, recent advances paved the way for the synthesis of colloidal dumbbells [1–4], ellipsoids [5], platelets [6] and colloidal clusters with polyhedral geometries [7–9]. If the mechanism of driving particle growth into an anisotropic direction is well understood, the acquired knowledge can be used to create particles with directional or site-specific physical properties originating from a specified particle shape. Examples are patchy particles [10] or Janus-type colloids, whose phase behavior and superstructure formation are governed by directional interactions [2]. Such systems therefore promise exciting opportunities in creating hierarchical organized synthetic materials [11–13].

Dumbbell-shaped polymer colloids are an interesting class of particles that can be synthesized at the gram scale and at a high degree of homogeneity in size and shape [3]. These particles can be thought of as anisotropic colloids with shapes reminiscent of space-filling models of diatomic molecules ("colloidal oxygen molecules"). Their particular shape, configuration and symmetry is responsible for a rich phase behavior with regard to superstructures built from those anisotropic particles [14, 15]. Their assembly has recently been investigated in some detail [16].

The synthesis of dumbbell-shaped polymer particles is based on seeded emulsion polymerization. This strategy was pioneered by El-Aasser and co-workers [17]. Cross-linked polystyrene seed particles of uniform spherical shape were swollen with monomer. Phase separation during seeded

✉ Alexander Wittemann
alexander.wittemann@uni-konstanz.de

[1] Colloid Chemistry, Department of Chemistry, University of Konstanz, Universitaetsstrasse 10, 78464 Constance, Germany

[2] Nanostructure Laboratory, University of Konstanz, Universitaetsstrasse 10, 78464 Constance, Germany

polymerization results in the formation of a liquid monomer protrusion attached to the seed particle [4]. Finally, polymerization of the protrusion yields a solid bulb permanently attached to the seed. The particles thus obtained have a shape that resembles two interpenetrating spheres and are thus referred to as dumbbell or snowman particles [1].

The formation of a liquid protrusion followed by a solidification is thus responsible for driving particle growth into an anisotropic direction giving rise to colloidal dumbbells. Dufresne and co-workers extended this strategy to non-cross-linked seed particles [3]. A particular coating on the seeds was used to modify the wettability of the seed surface with monomer. Hydrophilic groups at the seed surface decrease the swelling capacity of the seeds and thus facilitate the formation of liquid protrusions. Furthermore, the degree of surface hydrophilicity established during seed synthesis provides control on the contact angle between particle and monomer protrusion [4]. The contact angle influences the shape of the protrusion, and consequently the shape of the dumbbell particles.

The formation of a liquid protrusion attached to the seed is explained by the interplay of three different contributions of the free energy. The free energy of mixing of the monomer with the polymer is the only contribution that promotes swelling of the seed into a spherical cross-linked polymer network. In contrast, the other two contributions, namely minimization of the elastic energy of the swollen network and surface tension, facilitate formation of a liquid protrusion [4].

Although the mechanism and important experimental parameters have been investigated in some detail in similar systems [4], a direct *in-situ* analysis and visualization of the formation of liquid protrusions has not yet been achieved. We thus present the to the best of our knowledge first micrographs of liquid monomer droplets attached to polymeric seed particles. Cryogenic transmission electron microscopy (cryo-TEM) after rapid plunge vitrification allows for direct observation of colloids in aqueous media and therefore in states close to the ones in liquid dispersion [18–21]. In the recent past, much efforts were devoted to open electron microscopy and cryogenic conditions to new areas within colloid science. This includes the investigation of nanoemulsion droplets [22, 23], gas nanobubbles [24], silica-loaded miniemulsion droplets [25], and the growth of polystyrene nodules on silica seeds [26]. Inspired by these efforts, cryo-TEM is applied in the following to specifically explore liquid protrusions emerging from monomer swollen polymer seed particles (Fig. 1). Key parameters are the temperature and the monomer-to-seed volume ratio $V_m/V_{p.}$ In the latter quantity, V_m denotes the theoretical volume of polymer that could be expected from the added monomer. In other words, the volume of the polymer lobe resulting from the monomer protrusion can be estimated if V_m is divided by the total number of seed particles. V_p is the total volume of seed particles. The ratio V_m/V_p thus provides information on the relative volumetric dimensions of the two lobes of the dumbbells obtained after polymerization of the liquid protrusions. Hence, symmetric dumbbells are to be expected if $V_m/V_p = 1$. Both quantities, temperature and V_m/V_p thus substantially influence the interplay of the above-mentioned three thermodynamic contributions involved in the formation of liquid protrusions grown from monomer-swollen polymer particles.

Materials and methods

Chemicals

Trimethoxysilylpropylacrylate (TMSPA, 98%), potassium persulfate (KPS, ≥ 99%), sodium 4-vinylbenzesulfonate (NaSS, 99%), methyl-methacrylate (MMA, 99%) and azobisisobutyronitrile (AIBN, 98%) were purchased from Sigma-Aldrich and used as received. Styrene (99%, Merck) was passed over a column filled with inhibitor remover (for removing tert-butylcatechol; Sigma-Aldrich) before use. Sodium dodecylsulfate (SDS, ≥ 99%) was purchased from Carl Roth. Deionized water (resistivity ≥ 18 MΩcm) obtained from a reverse osmosis water purification system (Millipore Direct 8) was used throughout all experiments.

Synthesis of polystyrene (PS) particles

All syntheses were performed in three-necked flasks, which were equipped with a precision glass stirrer (KPG) with PTFE stirring blade, a reflux condenser, and a septum cap. The size of the reaction vessel is denoted in the individual sections of each synthesis.

For the synthesis of PS particles, a 2L flask was charged with SDS (1.9537 g, 6.775 mmol) dissolved in deionized water (1259.38 g). The reaction mixture was kept under nitrogen atmosphere while stirring at 250 rpm. Styrene (201.19 g, 1.932 mol) was passed over a column filled with inhibitor remover and degassed before the monomer was added to the SDS solution in the reaction vessel. The reaction mixture was heated up to 80 °C in a water bath before the initiator KPS (1.9202 g, 7.103 mmol; dissolved in 40 g deionized water) was added. The reaction mixture was kept at 80 °C for another term of 8 h. The dispersion was cooled to room temperature and filtered through glass wool to remove any particle agglomerates.

Synthesis of PS-co-PTMSPA particles

A dispersion of PS particles (124.27 g, 16% (m/m)) was mixed with deionized water (58.52 g) and charged into a

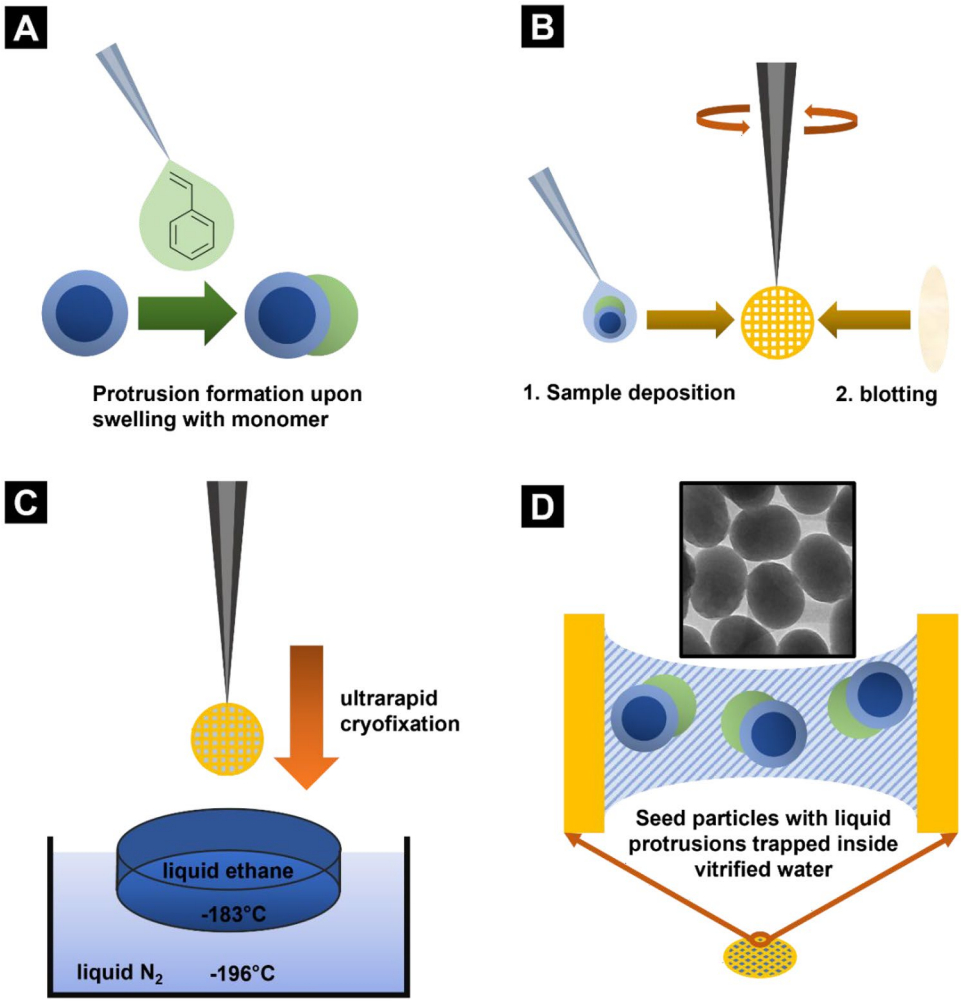

Fig. 1 Schematic visualization of the investigation of polymer particles with monomer protrusions. **A** Monomer is added to aqueous suspensions of polymer particles bearing a surface coating which limits the wettability with the monomer. The interplay of the free energy of mixing of polymer with monomer, the elastic energy of the polymer chains, and minimization of surface tension may promote segregation between monomer and polymer, thus yielding liquid protrusions attached to the polymer seeds. **B** The dispersion of seed particles bearing protrusions is applied onto a copper grid and blotted with filter paper on both sides to produce a thin film of water in which the colloidal species are embedded. **C** The TEM grid is plunged into liquid ethane at its freezing temperature yielding a vitrified specimen that can be transferred to the cryo holder of the electron microscope. **D** Cryofixation yields a thin film of vitrified water hosting the colloidal particles. Due to constraints in terms of space, the polymer colloids are preferably oriented with their long axis geared towards the direction of the film

250-mL three-necked flask. The mixture was kept under nitrogen atmosphere and stirred at 200 rpm. Styrene (16.67 g, 0.16 mol) was passed through a column filled with inhibitor remover and mixed with TMSPA (168 mg, 0.717 mmol) and AIBN (64.4 mg, 0.392 mmol). The initiator/monomer mixture was degassed and added to the reaction apparatus under stirring. Afterwards the reaction mixture heated up to 70 °C in an oil bath and kept at that temperature for another term of 8 h.

Synthesis of dumbbell-shaped particles with two polystyrene lobes

A 250-mL three-necked flask was charged with a NaSS solution (35.5 mg, 0.172 mmol; dissolved in 132.7 g of deionized water). An aqueous dispersion of PS-co-PTMSPA particles (41.35 g, 12.02% (m/m)) was added under stirring (200 rpm) and under nitrogen atmosphere. Styrene (5.07 g, 48.7 mmol) was passed through a column filled with inhibitor remover, mixed with AIBN (34.3 mg, 0.209 mmol) and degassed. Afterwards the monomer/initiator mixture was added to the reaction mixture and heated up to 70 °C in an oil bath. After a reaction time of 8 h the dispersion was cooled to room temperature and filtered through glass wool.

Synthesis of dumbbell particles with dissimilar lobes

A 250-mL three-necked flask was charged with a NaSS solution (29.8 mg, 0.144 mmol; dissolved in 100.0 g of deionized water). An aqueous dispersion of PS-co-PTMSPA particles (29.8 g, 12.02% (m/m)) was added under stirring (200 rpm) and under nitrogen atmosphere. MMA (4.09 g, 40.9 mmol) was passed through a column filled with inhibitor remover, mixed with AIBN (25.3 mg, 0.154 mmol) and degassed. The monomer/initiator mixture was added to the reaction mixture and heated up to 70 °C in an oil bath. After a reaction time of 8 h the dispersion was cooled to room temperature and filtered through glass wool.

Evolution of colloidal dumbbells over time

During the synthesis of dumbbells with two polystyrene lobes (described above), samples of 1 mL were taken from the reaction mixture at different polymerization times and quenched immediately in a bath of iced water. Each of the samples was partitioned into aliquots of 500 µL. The first aliquot was subject to a gravimetric analysis in order to determine the monomer conversion as of the time the sample was taken. To this end, the weight of the dispersion was determined on a precision scale (CPA324S, Sartorius Weighing Technology GmbH, Göttingen, Germany). Then the specimen was dried overnight at 80 °C in a drying cabinet (Venti-Line vl 53, VWR International GmbH, Darmstadt, Germany). The weight of the dried specimen was measured to determine the weight loss during drying. The latter quality was used to calculate the monomer conversion.

The second aliquots of 500 µL were extensively purified by dialysis. For the first 30 min of dialysis, the water was changed every 5 min to remove the unreacted monomer. The dialysis was continued for a total of 6 h. Minute amounts of the purified dispersions were dried on a silicon wafer and sputtered with 4 nm thick layer of platinum. Field-emission scanning electron micrographs (FESEM) were taken on a CrossBeam 1540 XB microscope (Carl Zeiss AG, Oberkochen, Germany) operating at 3 kV to observe the partially polymerized protrusions during dumbbell synthesis. In addition, further quantities of 100 µL purified dispersion were used to determine the average size of the polymer particles by differential centrifugal sedimentation (DCS). Since the FESEM and DCS analyses were performed after removal of residual monomer, the evolution of particle growth during seeded polymerization could be investigated (Fig. 5).

Cryogenic transmission electron microscopy

Cryo-TEM micrographs were taken on a Jeol JEM-2200FS HR-TEM operating at an acceleration voltage of 200 kV and on a Zeiss Libra 120 TEM operating at 120 kV. The chamber of the cryo-plunger (Leica EM GP) was heated to the desired temperature and set to 95% humidity to prevent rapid evaporation of the thin water film [27].

Preparation of cryo-TEM formulations

Samples were prepared by swelling aqueous suspensions of seed particles with either styrene or MMA at V_m/V_p ratios of 1.02 and 3.00. In addition to samples prepared at room temperature, further samples were prepared at an initial temperature of 60 °C. The latter temperature was chosen to perform experiments as close as possible to the temperature used in seeded polymerizations while still keeping the humidity at a constant level during preparation of cryo-TEM specimen. The exact compositions of the formulations are given in Table S1. The dispersion of PS-co-PTMSPA particles (12.02% (m/m)) was diluted with deionized water to a concentration of 0.1% (m/m). Either styrene or MMA of the desired volume together with minute amounts of sodium 4-styrene sulfonate were added. The charged comonomer was also used in the actual dumbbell synthesis to stabilize the newly formed lobes electrostatically and prevent collision-related fusion [3]. The Cryo-TEM experiments were carried out in absence of initiator to exclude polymerization during preparation of cryo-TEM specimen. To ensure thorough mixing, the dispersions were vortexed for 5 min. The samples were transferred to an oven and kept at either 25 °C or 60 °C for 30 min.

Preparation of cryo-TEM specimens

Specimens were prepared either on Cu-Lacey carbon grids with 400 mesh or on bare copper grids with 300 mesh, both purchased from Plano. The practical difference among the two sets of grids lies in the film thickness of vitrified water traversing either larger (cooper grid) or finer meshes (Cu-Lacey carbon grid). It turned out that even the finer mesh sizes of Lacey carbon films had no adverse effect in getting the colloidal particles embedded into the film of vitrified water.

2 µL of the dispersion was added to each side of the grid, blotted with filter paper, and plunged into liquid ethane at its freezing point (-183 °C) cooled in a liquid nitrogen bath. Under these conditions, the suspension is vitrified virtually instantaneously [23]. This procedure ensures preservation and fixation of liquid protrusions, allowing studies of their size and shape. Care was taken not to freeze the liquid ethane [28]. The specimen was then transferred to the electron microscope under cryogenic conditions and micrographs were taken within less than one hour. It should be noted that the specimens were kept at liquid nitrogen temperature throughout the transfer to the electron microscope and the measurement. A schematic illustration of the process is shown in Fig. 1.

Image analysis

The method for measuring seed particle and protrusion diameters via the program ImageJ is shown in Fig. S1 of the SI. The Cryo-TEM analyses were based on several hundreds of particles to ensure robust results. An overview of the amounts of monomer, particles and water for each experiment can be found in the SI (Table S1).

Results and discussion

Dumbbell particles with similar and dissimilar lobes obtained from seeded polymerizations

Along the lines given in Ref. [3], dumbbell-shaped polymer particles were prepared by seeded polymerization carried out at a temperature of 70 °C. Figure 2A shows a TEM micrograph of the polystyrene particles used as seeds. The spherical latex particles are bearing a thin hydrophilic surface layer resulting from copolymerization of styrene with the silane monomer TMPSA. As already mentioned, the surface layer plays an important role in limiting the swelling of the seed particles with monomer thus facilitating the formation of liquid protrusions. The PS-co-PTMPSA particles exhibit a narrow size distribution (Fig. S2), which is essential to obtain uniform dumbbell particles. The latter ones were obtained by swelling of the seed particles with monomer. In addition, small amounts of a charged comonomer (NaSS) were added to stabilize the polymer lobes grown from the monomer protrusions. Although the synthesis route was established for dumbbell particles with two polystyrene lobes of similar sizes [3, 16], it has turned out that the concept can be extended to the synthesis of dumbbell particles with lobes made from two different materials. For this purpose, a second seeded polymerization was performed to obtain dumbbell-shaped hybrid particles. One half of the particles is made from polystyrene, whereas the other half is made from PMMA. Both sets of dumbbells particles, the ones with two polystyrene lobes and those with two dissimilar lobes had narrow sizes distributions (Figs. 2B & C, S3). It has to be noted that full conversion from spherical seeds to dumbbell-shaped colloids was observed in both seeded polymerizations. TEM micrographs did not show any seed particles that preserved their spherical shape. This clearly shows that the experimental conditions during the polymerization routine facilitate formation a monomer protrusion on all the seed particles. In the following, detailed investigations by cryo-TEM were carried out aiming at fundamental insights into the formation of liquid protrusion as transient states during anisotropic growth of polymer colloids.

Investigation of monomer protrusions

Figure 3 shows seed particles swollen with styrene under different conditions. The protrusions attached to the seed particles were clearly visible on all micrographs. Dumbbell-shaped colloids with lobes of dissimilar sizes and contrasts were observed. This underlines the asymmetric swelling behavior of the surface-functionalized seeds yielding liquid protrusions. Remarkably, the samples comprised both colloidal spheres and asymmetric dumbbells, which clearly indicates coexistence of spherical swollen seed particles and seeds bearing protrusions. In the latter case, a clear distinction between seed and protrusion could be made because the smaller lobes had a smaller average diameter of 143 nm (at $V_m/V_p = 1.02$ and 25 °C) than the seeds before swelling (158 nm). On the contrary, the big lobes had a significantly larger diameter of 180 nm than the seeds before swelling. It is thus apparent that the small lobe is the liquid protrusion, while the big lobe refers to a seed swollen with monomer. Notwithstanding the surface hydrophilicity provided by the TMPSA coating at the seed surface, a significant swelling from an initial size of 158 nm to 180 nm was observed at a monomer-to-seed volume ratio of 1.02. Interestingly, a coexistence of swollen seeds and seeds carrying protrusions was also found at a larger ratio of $V_m/V_p = 3.00$. Irrespective of

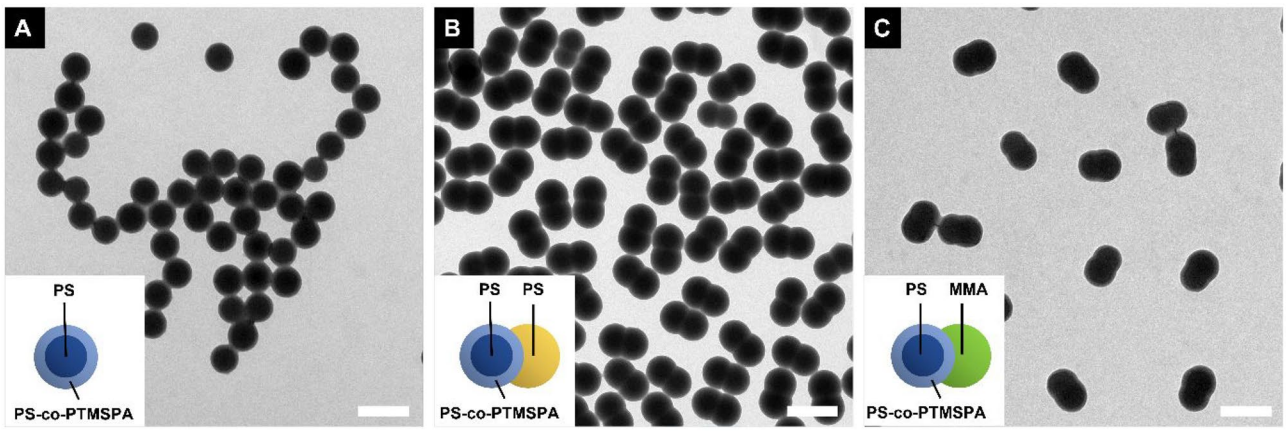

Fig. 2 TEM micrographs of seed particles and colloidal dumbbells. **A** Seed particles with core–shell character. **B** Colloidal dumbbells composed of two polystyrene lobes. **C** Hybrid material colloidal dumbbells with a polystyrene and a PMMA lobe. The scale bar is equivalent to 200 nm. Inset shows schematic representation of the material composition of colloids

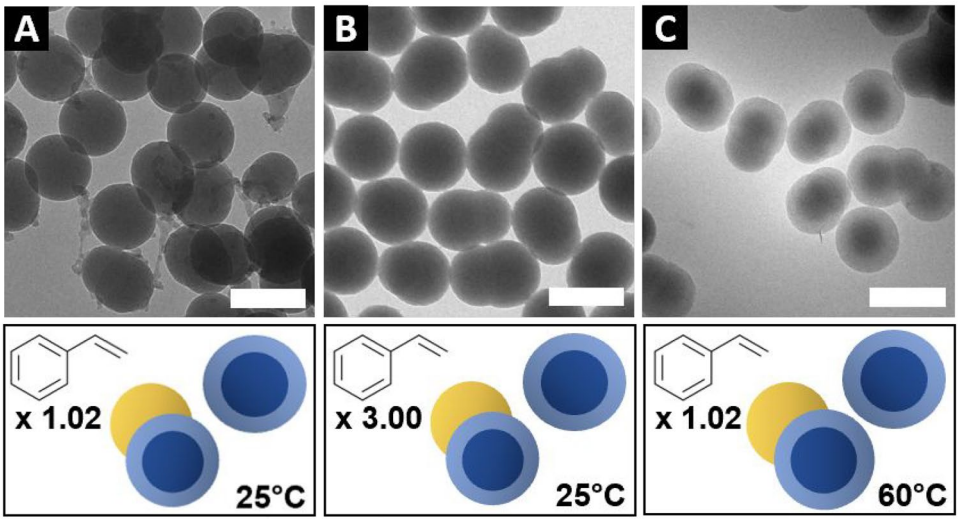

Fig. 3 Cryo-TEM micrographs of seed particles swollen with styrene for different monomer-to-particle volume ratios and temperatures. **A** $V_m/V_P = 1.02$, 25 °C. **B** $V_m/V_P = 3.00$, 25 °C. **C** $V_m/V_P = 1.02$, 60 °C. The scale bar is equivalent to 200 nm

the threefold increase in monomer volume, there was still a considerable portion of swollen seed particles (30%) that did not develop a monomer protrusion. The average sizes of seeds and protrusions had only increased by less than 4 nm (Table 1). This corresponds to an average increase in protrusion volume of 8%. The most important difference is however that the number ratio of seeds with protrusions to those without protrusions changed significantly with rising V_m/V_p ratio. At $V_m/V_p = 1.02$, 60% out of 403 seed particles studied were carrying liquid protrusions. As a result of the threefold increase in monomer volume ($V_m/V_p = 3.00$), the yield of seeds with protrusion rose to 70%. This suggests that the interplay of free energy of mixing of the monomer with the polymer, free elastic energy of the swollen network and surface tension has substantially shifted towards formation of liquid protrusions rather than bare swelling of the seeds.

The coexistence of seed particles with and without protrusions was surprising because only dumbbell particles were obtained from seeded emulsion polymerizations at the V_m/V_p ratios probed in the cryo-TEM experiments. Furthermore, the cryo-TEM micrographs clearly indicate that the protrusions are quite uniform in size as soon as they are formed. These two striking observations were made on the basis of formulations prepared at room temperature, whereas the actual polymerizations were carried out at 70 °C. It is to be expected that temperature strongly affects the thermodynamic contributions that govern the formation of liquid protrusions from monomer-swollen seeds. Nonetheless, segregation into two states without any intermediate states may sound a bit contradictory at a first sight. Current understanding of protrusion formation is based on pure thermodynamics. The thermodynamically preferred state is the one which has the lowest free energy. The latter is the sum of the free energy of mixing of the monomer with the polymer, the elastic energy of the swollen network, and surface tension. The observation of a bi-state behavior suggests that there is a kinetic barrier that may hamper or delay formation of a protrusion. Once this obstacle is overcome, instant formation of the protrusion will occur to the fullest extent predicted by the interplay of the thermodynamic contributions. This instant change from swollen seeds to a protrusion-bearing particle is in accordance with the absence of a distribution of protrusion sizes. The latter cannot be

Table 1 Calculation of swelling ratios. H_V denotes the volume swelling ratio and H_w the weight swelling ratios. The value for d_0 was assumed to be 158 nm for all samples. N denotes the number of evaluated particles. See Eqs. (1) and (2). Size distributions of the swollen seeds are shown in Figs. S4 and S5 of the ESI

Sample	Monomer	V_M/V_P	T [°C]	Species	d [nm]	H_V	H_W	N
1	styrene	1.02	25	spherical	186 ± 9	1.631	1.545	81
				protrusion-bearing	180 ± 8	1.479	1.413	58
2	styrene	3.00	25	spherical	187 ± 7	1.658	1.574	82
				protrusion-bearing	184 ± 4	1.579	1.500	78
3	styrene	1.02	60	spherical	183 ± 7	1.554	1.478	64
				protrusion-bearing	180 ± 3	1.479	1.413	111
4	MMA	1.02	25	spherical	171 ± 5	1.268	1.239	124
5	MMA	3.00	25	protrusion-bearing	162 ± 3	1.078	1.070	96
6	MMA	1.02	60	spherical	175 ± 9	1.359	1.320	93

observed because it is likely that protrusion growth once the kinetic hindrance is overcome proceeds on a much smaller time scale than the one probed by cryo-TEM. The low dispersity of the protrusions is related to the narrow size distribution of the seed particles (Fig. S2). The latter species can be regarded as a reservoir from which the monomer is taken to build the protrusion. This hypothesis is confirmed by syntheses that yield dumbbells with equal-sized lobes. Occasionally, dumbbell particles with sizes significantly below average were observed. Even these species grown from smaller seeds had equal-sized lobes. This is a clear indication that the size of the protrusion and related to this the size of the newly grown lobe is directly related to the seed volume. As a practical benefit, it follows that the dispersity of the seed particles is automatically transferred to the protrusion and to the lobes formed thereof.

Effect of higher temperature on protrusion formation

As outlined above, temperature is a key parameter that redefines the interplay among the three thermodynamic contributions responsible whether or not monomer protrusions are obtained. Given the fact that the actual polymerizations reactions carried out at 70 °C exclusively yield dumbbell particles, it is to be expected that elevated temperatures should facilitate the formation of protrusions. To test this hypothesis, a further sample with a V_m/V_p ratio of 1.02 was prepared at a temperature of 60 °C. The temperature had to be set lower than the actual polymerization temperature of 70 °C because the device required for the cryo-fixation cannot be operated reliably at a temperature above 60 °C. As compared to the observations at room temperature, notable increases in both the sizes of the swollen seed particles as well as the liquid protrusion were visible. At 60 °C, the seeds with a protrusion (180 nm) and those without protrusion (183 nm) had similar sizes within the limits of experimental errors. The average size of the protrusions was 152 nm, indicating enhanced uptake of monomer with increasing temperature. Seeds without protrusion were found at 60 °C as well, albeit at a much smaller proportion. 78% of the seed particles were carrying a monomer protrusion. It is thus to be expected that their proportion will be even larger during the actual dumbbell synthesis carried out at 70 °C [3]. This is reflected by the fact that only dumbbell particles were obtained after complete conversion of the monomer at this elevated temperature [16].

Ethane at its freezing point is often used as the cryogen of choice. Reasons for this preference are the high heat transfer coefficient and the low freezing point (-183 °C). These conditions enable rapid cryo-fixation in a state close to the native one in suspension [29]. A point to be made is that liquid ethane dissolves many organic materials and is thus not believed to be suitable for oil-rich samples [21, 22]. It cannot be ruled out that a part of monomer had been removed by the liquid ethane in this study. On the other hand, it can be assumed that ethane as an efficient cryogen ensures rapid vitrification of the continuous water phase, thus minimizing dissolution of dispersed emulsion droplets. Proof of this can be seen by the frequency of occurrence and the spatial dimensions of styrene protrusions observed at 60 °C and $V_m/V_p = 1.02$. Nevertheless, further studies including other cryogens such as liquid nitrogen are necessary for subsequent clarification.

Swelling of the seed particles with monomer

To compare the swelling of the seed particles to known literature values the swelling ratios were determined from the dimensions of the imaged particles. The swelling ratios by volume (H_V) and weight (H_w) were calculated from the diameters of the seed particles before (d_0) and after (d) swelling using the following equations [30]:

$$H_V = \left(\frac{d}{d_0}\right)^3 \tag{1}$$

$$H_w = \left(H_V - 1\right)\left(\frac{\delta_m}{\delta_P}\right) + 1 \tag{2}$$

Here δ_m describes the density of the monomer (styrene: 0.909 g cm^{-3}, [31] MMA: 0.94 g cm^{-3} [32]) and δ_P the density of the polymer seeds (1.054 g cm^{-3} [33]). Table 1 gives an overview of the swelling ratios for all samples. When comparing the weight swelling ratios H_w of styrene-swollen seed particles, the ratios were smaller (1.479–1.628) for all samples than the known literature values (2–3) [30]. This confirms the reduced swelling capacity of swollen seeds as well as seeds bearing protrusions induced by the hydrophilic shell of the seed particles proposed by Dufresne et al. in their original paper [3].

Observations made with methyl-methacrylate as monomer

Swelling experiments with the same seed particles were performed with methyl-methacrylate (MMA) instead of styrene to investigate protrusion formation of a more polar monomer in the formation of hybrid material dumbbells. Figure 4 shows cryo-TEM micrographs of the resulting samples. In contrast to seeds swollen with styrene, the samples at $V_m/V_p = 1.02$ showed almost no protrusions when swollen with MMA. Only 0.5% of the evaluated seeds had an attached liquid droplet. Seed size increased from 158 to 171 nm in swollen state, indicating a slightly

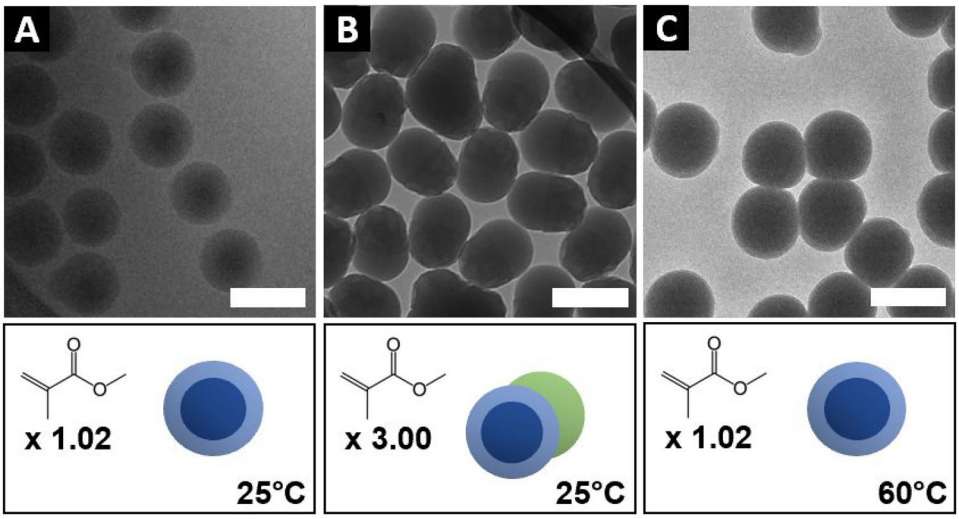

Fig. 4 Cryo-TEM micrographs of seed particles swollen with MMA at different monomer-to-particle volume ratios and temperatures. **A** $V_m/V_P = 1.02$, 25 °C. **B** $V_m/V_P = 3.00$, 25 °C. **C** $V_m/V_P = 1.02$, 60 °C. The scale bar is equivalent to 200 nm

smaller swelling capacity for MMA. When increasing the monomer-to-particle ratio to $V_m/V_P = 3.00$, there was an enormous increase in protrusion formation. Now, 94% of the evaluated swollen seed particles showed a protrusion. At the same time the diameter of the swollen seeds decreased when compared to the sample with $V_m/V_p = 1.02$ to a value of 162 nm. The diameter of the protrusions was found to be 154 nm on average.

Protrusions formed upon swelling with MMA did not show a pronounced indentation between the two lobes of the dumbbell shape (see Fig. 4B). This can be explained by a smaller contact angle between the hydrophilic surface layer of the seed and the polar monomer MMA.

Seed particles swollen with MMA showed smaller H_w values (1.070–1.320) than seeds swollen with styrene (Table 1). These values are also smaller than those determined by Gonzalez-Ortiz et al. [34] This again underpins that the TMPSA coating at the seed surface substantially reduces the extent of seed swelling and thus promotes the formation of a liquid protrusion.

The effect of higher temperature on the seed particle/MMA system was investigated as well. To this end, a sample prepared at a ratio of $V_m/V_p = 1.02$ and 60 °C was explored. The proportion of seeds showing protrusions increased slightly to 2% when compared to the sample prepared at 25 °C. This is consistent with previous work indicating little temperature dependence below saturation swelling with MMA [35]. The diameter of the swollen seed was determined to be 175 nm. The determination of this quantity is however prone to experimental uncertainty, inasmuch as the particles in this sample appear deformed which may indicate an early stage of protrusion formation (see Fig. 4C).

Monomer partioning in suspension and its impact on protrusion formation

It should be noted that there is a clear mismatch between the total volumetric gain of the particles upon swelling and formation of protrusions and the total volume of monomer added. This means that not all the monomer is initially absorbed by the seed particles. It becomes evident that residual monomer must be present. Another possibility is the partitioning of the excess styrene between the vitrified dispersion and the liquid ethane during plunging the sample into the cryogen. As liquid ethane is known to draw hydrocarbons from samples [21]. This possibility cannot be completely ruled out, although it does not seem to prevent protrusion formation.

Based on the solubility of both monomers in water at room temperature (styrene: 0.3 g/L [36] and MMA: 1.5 g/L [37]) and at 60 °C (styrene: 0.237 g/L [38] and MMA: 2.25 g/L [38]), a simple balance calculation can be made. The amounts of monomer inside the particles and the excess monomer for each sample is summarized in Table 2. In the case of swelling with styrene, the amount of excess monomer is always greater than the solubility of styrene in water, further supporting the idea of the presence of monomer droplets. Most of residual monomer is presumably present as microscale droplets, which serve as a reservoir, providing further monomer supply during the polymerization. This is also reflected by the final size of the polymer lobes grown

Table 2 Partitioning of monomer bound by the seed particles (by swelling and protrusion formation) and free monomer in solution: V_{diff} denotes the volume increase resulting from swelling and formation of a protrusion. This quantity was used to calculate the total amount of monomer trapped inside or attached to the seed particles as protrusions. *N* denotes the number of evaluated particles

Sample	Monomer	V_M/V_P	T [°C]	V_{diff} [M10^{-21} m^{-3}]	Monomer bound [g L^{-1}]	Free monomer [g L^{-1}]	N
1	styrene	1.02	25	8.3821	0.497	0.503	139
2	styrene	3.00	25	9.9627	0.603	2.397	160
3	styrene	1.02	60	9.7975	0.593	0.407	175
4	MMA	1.02	25	4.7748	0.289	0.745	124
5	MMA	3.00	25	17.2819	1.046	2.056	96
6	MMA	1.02	60	6.2122	0.376	0.658	93

during seeded emulsion polymerization. Their average size of 171 nm exceeds the one of the liquid protrusions.

The situation is different in the case of MMA swelling, where for both samples with $V_m/V_p = 1.02$ the amount of excess monomer was lower than the solubility of MMA in water. These samples did hardly show any protrusions. Only the sample with a V_m/V_p ratio of 3.00 had an amount of excess monomer exceeding the solubility of MMA in water. Here a large increase in protrusion formation is observed leading to the assumption, that the formation of a liquid droplet on the seed particle surface requires an excess of the monomer above its solubility in the aqueous phase. Interestingly, the development of a dumbbell shape is achieved in polymerizations at $V_m/V_p = 1.02$ as well, pointing to the soluble portion of the MMA as a reservoir for monomer supply during seeded polymerization.

Anisotropic particle growth over time mediated by monomer protrusions

Parallel to the investigations by cryo-TEM, formation and growth over time of solid polymer lobes that result from the liquid monomer protrusions were explored. This measure adds a complementary view on intermediate stages during formation of dumbbell-shaped polymer particles. The work performed concentrated on seeded heterophase polymerizations that result in colloidal dumbbells with two polystyrene lobes that have approximately the same size.

Samples were taken from the reaction mixture at various stages during seeded polymerization. Figure 5A shows the evolution of monomer conversion during the dumbbell synthesis. The latter is calculated based on the weight loss that can be determined after removal of the volatile

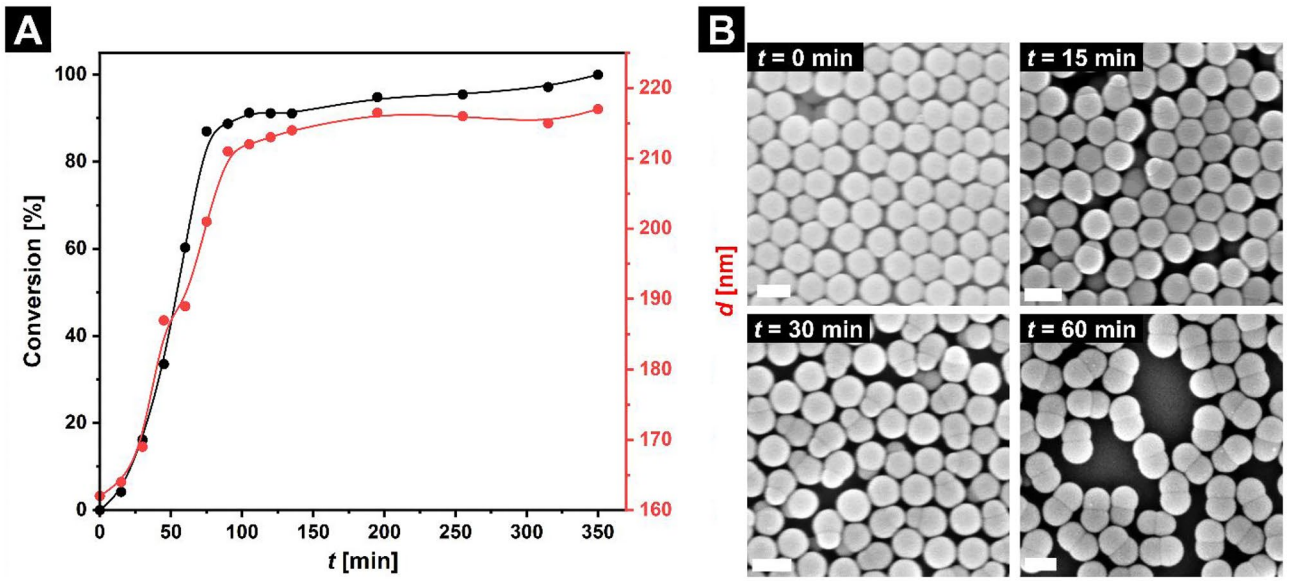

Fig. 5 Temporal evolution of monomer conversion, particle size, and lob sizes during the synthesis of colloidal dumbbells mediated by monomer protrusions attached to spherical seed particles. **A** Monomer conversion (black dots) compared to the growth in average particle sizes determined by DCS (red dots). Solid lines serve as a guide to the eye. **B** FESEM micrographs of samples taken during synthesis at various polymerization times. Unreacted monomer was removed by exhaustive dialysis against deionized water. Scale bars are 200 nm

monomer. The data on monomer conversion is superimposed by the average sizes of the particles at the same stage of the polymerization. The average particle sizes were measured by DCS. The size evolution follows the monomer conversion with most of the growth occurring during the first 60 min of the seeded polymerization. As a complementary measure, FESEM micrographs were taken from these samples (Fig. 5B). They illustrate the growth of a second polymer lobe from the monomer protrusion attached to the seed particle upon the first 60 min of the reaction. The latter further highlight that the dumbbell formation is virtually completed after a reaction period of 60 min, which corresponds a monomer consumption of about 50%. At this stage of the polymerization, the freshly formed lobe has reached a size comparable to the seed particle that promoted its formation. Further growth is equally distributed over both lobes as monomer conversion progresses slowly during later stages of the polymerization. Together with the knowledge of protrusion formation obtained by cryo-TEM analysis of similar samples, it can be concluded that growth of the new lobe proceeds preferentially inside the monomer protrusion attached to the seed particle and, consequently, away from the monomer-swollen seed particle. As the polymerization continues, the new lobe gains in size, which is further promoted by swelling of both lobes thus ensuring continuous monomer supply. This leads to the assumption of a virtually symmetrical dumbbell shape already if half of the monomer is converted into its polymer. Further investigation is required to validate this mechanism further. Nonetheless, the results from cryo-TEM clearly demonstrate that the protrusion acts not only as a growth site, but also as a monomer reservoir during the synthesis of dumbbell-shaped polymer particles.

Conclusion

Monomer droplet-based synthesis has proven as a viable route to produce anisotropic polymer particles at large scale. An important example is the formation of dumbbell-shaped polymer particles. Evolution of the anisotropic particle shape is mediated by solid–liquid separation during seeded heterophase polymerizations resulting in polymerizable monomer protrusions. Capturing these transient states during shape evolution requires an analytical tool that not only provides resolution at the nanoscale, but also instantaneous fixation in a state as close as possible to the native one. This study has shown that cryo-TEM is an ideal answer to this problem. It reveals the swelling behavior of the seed particles with respect to different monomers. Furthermore, evolution of liquid protrusions that emerge from the monomer-swollen seed particles can be studied under different experimental conditions. On account of ultrahigh cooling rates (approaching 1,000,000 K/s [23]), even transient states at elevated temperatures can be captured.

In general, we expect further work on phase separation and liquid–solid demixing in nanoscale objects to follow, as well as adaptation of the method to other colloidal phenomena that involve transient states.

Supplementary Information The online version contains supplementary material available at https://doi.org/10.1007/s00396-022-05000-1.

Acknowledgements Technical support from the Nanostructure Laboratory (nano.lab) and the Particle Analysis Centre (PAC) at the University of Konstanz is gratefully acknowledged.

Funding Open Access funding enabled and organized by Projekt DEAL. This research was funded by the DEUTSCHE FORSCHUNGSGEMEINSCHAFT within SFB 1214/B4.

Data availability The datasets generated during the study are available from the corresponding author on reasonable request.

Declarations

Conflicts of interest The authors disclose financial or non-financial interests that are directly or indirectly related to the work submitted for publication.

References

1. Mock EB, De Bruyn H, Hawkett BS, Gilbert RG, Zukoski CF (2006) Synthesis of anisotropic nanoparticles by seeded emulsion polymerization. Langmuir 22:4037–4043. https://doi.org/10.1021/la060003a
2. Kim J-W, Larsen RJ, Weitz DA (2006) Synthesis of nonspherical colloidal particles with anisotropic properties. J Am Chem Soc 128:14374–14377. https://doi.org/10.1021/ja065032m
3. Park J-G, Forster JD, Dufresne ER (2010) High-yield synthesis of monodisperse dumbbell-shaped polymer nanoparticles. J Am Chem Soc 132:5960–5961. https://doi.org/10.1021/ja101760q
4. Van Ravensteijn BGP, Kegel WK (2017) Tuning particle geometry of chemically anisotropic dumbbell-shaped colloids. J Colloid Interface Sci 490:462–477. https://doi.org/10.1016/j.jcis.2016.11.045
5. Sickinger A, Mecking S (2021) Origin of the anisotropy and structure of ellipsoidal poly(fluorene) nanoparticles. Macromolecules 54:5267–5277. https://doi.org/10.1021/acs.macromol.1c00597
6. Morgen TO, Krumova M, Luttikhedde H, Mecking S (2018) Free-radical dispersion polymerization of ethylene with laponite

to polyethylene–clay nanocomposite particles. Macromolecules 51:4118–4128. https://doi.org/10.1021/acs.macromol.8b00440
7. Wang Y, Wang Y, Breed DR, Manoharan VN, Feng L, Hollingsworth AD, Weck M, Pine DJ (2012) Colloids with valence and specific directional bonding. Nature 491:51. https://doi.org/10.1038/nature11564
8. Hoffmann M, Wagner CS, Harnau L, Wittemann A (2009) 3d brownian diffusion of submicron-sized particle clusters. ACS Nano 3:3326–3334. https://doi.org/10.1021/nn900902b
9. Wagner CS, Fischer B, May M, Wittemann A (2010) Templated assembly of polymer particles into mesoscopic clusters with well-defined configurations. Coll Polym Sci 288:487–498. https://doi.org/10.1007/s00396-009-2169-y
10. Wolters JR, Verweij JE, Avvisati G, Dijkstra M, Kegel WK (2017) Depletion-induced encapsulation by dumbbell-shaped patchy colloids stabilize microspheres against aggregation. Langmuir 33:3270–3280. https://doi.org/10.1021/acs.langmuir.7b00014
11. Plüisch CS, Wittemann A (2013) Shape-tailored polymer colloids on the road to become structural motifs for hierarchically organized materials. Macromol Rapid Commun 34:1798–1814. https://doi.org/10.1002/marc.201300693
12. Jiang S, Chen Q, Tripathy M, Luijten E, Schweizer KS, Granick S (2010) Janus particle synthesis and assembly. Adv Mater 22:1060–1071. https://doi.org/10.1002/adma.200904094
13. Glotzer SC, Solomon MJ (2007) Anisotropy of building blocks and their assembly into complex structures. Nat Mater 6:557–562. https://doi.org/10.1038/nmat1949
14. Milinković K, Dennison M, Dijkstra M (2013) Phase diagram of hard asymmetric dumbbell particles. Phys Rev E 87:032128. https://doi.org/10.1103/PhysRevE.87.032128
15. Marechal M, Dijkstra M (2011) Colloidal hard dumbbells under gravity: Structure and crystallization. Soft Matter 7:1397–1408. https://doi.org/10.1039/C0SM00589D
16. Stuckert R, Lüders A, Wittemann A, Nielaba P (2021) Phase behaviour in 2d assemblies of dumbbell-shaped colloids generated under geometrical confinement. Soft Matter 17:6519–6535. https://doi.org/10.1039/d1sm00635e
17. Sheu HR, El-Aasser MS, Vanderhoff JW (1990) Uniform non-spherical latex particles as model interpenetrating polymer networks. J Polym Sci A Polym Chem 28:653–667. https://doi.org/10.1002/pola.1990.080280315
18. Wittemann A, Drechsler M, Talmon Y, Ballauff M (2005) High elongation of polyelectrolyte chains in the osmotic limit of spherical polyelectrolyte brushes: A study by cryogenic transmission electron microscopy. J Am Chem Soc 127:9688–9689. https://doi.org/10.1021/ja0513234
19. Crassous JJ, Rochette CN, Wittemann A, Schrinner M, Ballauff M, Drechsler M (2009) Quantitative analysis of polymer colloids by cryo-transmission electron microscopy. Langmuir 25:7862–7871. https://doi.org/10.1021/la900442x
20. Kuntsche J, Horst JC, Bunjes H (2011) Cryogenic transmission electron microscopy (cryo-tem) for studying the morphology of colloidal drug delivery systems. Int J Pharm 417:120–137. https://doi.org/10.1016/j.ijpharm.2011.02.001
21. Kesselman E, Talmon Y, Bang J, Abbas S, Li Z, Lodge TP (2005) Cryogenic transmission electron microscopy imaging of vesicles formed by a polystyrene-polyisoprene diblock copolymer. Macromolecules 38:6779–6781. https://doi.org/10.1021/ma0510587
22. Guttman S, Kesselman E, Jacob A, Marin O, Danino D, Deutsch M, Sloutskin E (2019) Nanostructures, faceting, and splitting in nanoliter to yoctoliter liquid droplets. Nano Lett 19:3161–3168. https://doi.org/10.1021/acs.nanolett.9b00594
23. Klang V, Matsko NB, Valenta C, Hofer F (2012) Electron microscopy of nanoemulsions: An essential tool for characterisation and stability assessment. Micron 43:85–103. https://doi.org/10.1016/j.micron.2011.07.014
24. Hernandez C, Gulati S, Fioravanti G, Stewart PL, Exner AA (2017) Cryo-em visualization of lipid and polymer-stabilized perfluorocarbon gas nanobubbles - a step towards nanobubble mediated drug delivery. Sci Rep 7:13517. https://doi.org/10.1038/s41598-017-13741-1
25. Bourgeat-Lami E, Farzi GA, David L, Putaux JL, Mckenna TF (2012) Silica encapsulation by miniemulsion polymerization: Distribution and localization of the silica particles in droplets and latex particles. Langmuir 28:6021–6031. https://doi.org/10.1021/la300587b
26. Taveau J-C, Nguyen D, Perro A, Ravaine S, Duguet E, Lambert O (2008) New insights into the nucleation and growth of ps nodules on silica nanoparticles by 3d cryo-electron tomography. Soft Matter 4:311–315. https://doi.org/10.1039/B710137F
27. Weissenberger G, Henderikx RJM, Peters PJ (2021) Understanding the invisible hands of sample preparation for cryo-em. Nat Methods 18:463–471. https://doi.org/10.1038/s41592-021-01130-6
28. Cabra V, Samsó M (2015) Do's and don'ts of cryo-electron microscopy: A primer on sample preparation and high quality data collection for macromolecular 3d reconstruction. J Vis Exp 95:e52311. https://doi.org/10.3791/52311
29. Bachmann L, Talmon Y (1984) Cryomicroscopy of liquid and semi-liquid specimens: Direct imaging versus replication. Ultramicroscopy 14:211–218. https://doi.org/10.1016/0304-3991(84)90089-5
30. Gardon JL (1968) Emulsion polymerization. Vi. Concentration of monomers in latex particles. J Polym Sci A Polym Chem 6:2859–2879. https://doi.org/10.1002/pol.1968.150061015
31. Patnode W, Scheiber W (1939) The density, thermal expansion, vapor pressure, and refractive index of styrene, and the density and thermal expansion of polystyrene. J Am Chem Soc 61:3449–3451. https://doi.org/10.1021/ja01267a066
32. Fan W, Zhou Q, Sun J, Zhang S (2009) Density, excess molar volume, and viscosity for the methyl methacrylate + 1-butyl-3-methylimidazolium hexafluorophosphate ionic liquid binary system at atmospheric pressure. J Chem Eng Data 54:2307–2311. https://doi.org/10.1021/je900091b
33. Plüisch CS, Stuckert R, Wittemann A (2021) Direct measurement of sedimentation coefficient distributions in multimodal nanoparticle mixtures. Nanomaterials 11:1027. https://doi.org/10.3390/nano11041027
34. González-Ortiz LJ, López-Naranjo EJ, Guzmán Jiménez MH, Sánchez Peña MJ (2012) Swelling behavior of polystyrene particles with monomers commonly used in seeded emulsion polymerizations. Int J Polym Anal 17:444–457. https://doi.org/10.1080/1023666X.2012.696051
35. Maxwell IA, Kurja J, Van Doremaele GHJ, German AL, Morrison BR (1992) Partial swelling of latex particles with monomers. Makromol Chem 193:2049–2063. https://doi.org/10.1002/macp.1992.021930823
36. He Y, Jain P, Yalkowsky SH (2010) Handbook of aqueous solubility data. CRC Press, Boca Raton
37. World Health Organization, Programme I-O, for the Sound Management of Chemicals (1998) Concise international chemical assessment document. World Health Organization, Geneva
38. Chai XS, Schork FJ, Decinque A, Wilson K (2005) Measurement of the solubilities of vinylic monomers in water. Ind Eng Chem Res 44:5256–5258. https://doi.org/10.1021/ie0492303